

# The effect of surface constraints on the ordering of block copolymer domains

CHRIS S. HENKEE, EDWIN L. THOMAS

*Polymer Science and Engineering Department, University of Massachusetts, Amherst, Massachusetts 01003, USA*

LEWIS J. FETTERS

*Corporate Research - Science Laboratories, Exxon Research and Engineering Company, Annandale, New Jersey 08801, USA*

The effect of surfaces on the ordering of block copolymer microdomains has been studied by TEM observation of thin-film droplets. Poly(styrene butadiene) block copolymers exhibiting spherical, cylindrical and lamellar microdomain morphologies were formed by solvent evaporation on a carbon substrate, annealed above  $T_g$ , and stained with  $\text{OsO}_4$  prior to TEM observation. Samples with lamellar morphologies exhibited orientations of the lamellae in which the domains were either perpendicular to the substrate surface, or parallel to the substrate surface in which a layered structure resulted. Specimens in which cylinders were formed revealed sheets in which the cylinder axes lie parallel to the substrate, as well as parallel to each other. Stacking of such layers was observed, with exceptional registration between layers such that the cylinders in one layer were located over the inter-domain regions of the cylinders in adjacent layers. Specimens with spherical microdomain morphologies revealed a layer structure that consisted of hexagonally packed arrays of the spherical micelles. The stacking of layers of discrete thickness of all three types of microdomain morphology to produce the observed geometries indicates that the exterior of bulk samples may also exhibit such surface steps that reflect the ordering of the microdomains within the sample. Regardless of the microdomain type, all samples revealed a peripheral region in the thinnest area of the droplets in which the formation of the normal microdomain morphology (i.e. that of spheres, cylinders or lamellae) was inhibited. The uniform thickness of this region provides evidence that preferential segregation of the block component with the lowest surface energy takes place regardless of the sample composition.

## 1. Introduction

The morphology associated with the phase segregation that occurs in block copolymers has long been of interest. Previous morphological studies [1-9], as well as theoretical treatments [10-12] have investigated the nature of the three-dimensional microdomain structure that forms in bulk samples. From these studies, it is concluded that the equilibrium morphology is essentially determined by the volume fraction of the components present [1, 2]. If the minority component is less than about 20 vol %, spherical micelles of this constituent are formed. These micelles contain a core region where the minority component resides, surrounded by a corona composed of the majority constituent. If the volume percentage of the minority component is between 20 and 35, cylindrical microdomains are present; and finally, from 35 to 50 vol %, alternating lamellae of the two components are observed with symmetric results about 50%. Recently, an additional structure, that of the ordered bicontinuous double diamond structure (OBDD) has also been observed to exist in a small composition window that lies between the cylindrical and lamellar regimes

[13, 14]. The fundamental building block of the OBDD structure is an arrangement of four short cylinders of the minority component, joined together such that the cylinders are disposed towards the corners of a tetrahedron. The dividing surface between the two polymer phases in the OBDD morphology is best represented by a surface of constant mean curvature [13].

Under equilibrium conditions, the various microdomain types organize themselves into ordered arrays. For example, the spherical micelles order on to a bcc lattice [4, 15]. In the case in which cylindrical microdomains of the minority component are formed, a hexagonally packed array is observed. In the OBDD structure, the short cylinders join together to form two interwoven but unconnected lattices having diamond symmetry. In the case of lamellar microdomains, grains of regularly alternating lamellae of the two components are found.

For many of the applications for which block copolymers are used (adhesives, membranes, etc.) it is the surface properties of the block copolymer systems which are exploited. There have been several

studies that have investigated the surface structure of block copolymer samples. Experiments employing contact angle measurements, or spectroscopic techniques [16, 17], have indicated that the polymer block with the lowest surface free energy preferentially segregates to the surface of the sample. On the other hand, some spectroscopic techniques have provided evidence for the existence of isolated surface domains of blocks in polystyrene–poly(ethylene oxide) (PS–PEO) block copolymers. (It should be noted that in the PS–PEO system, the presence of a crystallizable component such as PEO may give rise to results that are different from those obtained with block copolymers consisting of amorphous constituents.) In addition, it must be kept in mind that in most of these experiments, solvent cast films were used. Such samples might be expected to be far from their equilibrium configuration.

The surface topography of polystyrene–polybutadiene (PS–PB) block copolymer samples has been studied by replication techniques [18, 19]. This replication technique first provided evidence that the surface exhibited topographic features that resembled ridges or “steps” for these solvent-cast films. A second set of experiments using optical microscopy has investigated the surface topography of constrained binary and ternary block copolymer–solvent systems [20]. For a polystyrene–polyisoprene block copolymer in a pentanedione–*n*-decane mixture, a terracing of the surface was observed at air–bubble interfaces.

Information on the presence and/or the size and shape of the domains associated with the surface region is difficult to obtain. One approach is to embed samples and microtome them in such a way as to intersect the surface region. TEM of these cross-sections can then reveal the arrangement of the domains at or near the surface [1, 21]. The early work of Kämpf *et al.* [1] concerned ultrathin (50 nm) solvent-cast films of PS–PB in which they observed cylinders of PS oriented in the plane of the film surrounded by two continuous layers of PB. They did not comment on the surface structure of the film since they noted the electron density of the PS phase was nearly the same as that of the embedding medium. Hasegawa and Hashimoto [21] also investigated the PS–PB system using cross-sectional microtomy and found what appeared to be preferential surface segregation of a thin continuous layer of PB. Other than these two experiments, previous work has not endeavoured to study the arrangement of the domains at or near the surface, or the change in the structure as one proceeds into the bulk of the sample. These are important questions, since the presence of a surface must necessarily modify the three-dimensional ordering of the domains.

In dealing with the surface regions of block copolymers, several important physical considerations arise. An idealized block copolymer–air interface is schematically illustrated in Fig. 1a. Several types of region can be defined progressing from the surface ( $z = 0$ ) into the interior of the sample. First, directly adjacent to the external surface, the molecular chains must be perturbed from their Gaussian statistics due to the geometric constraints imposed upon them by the free

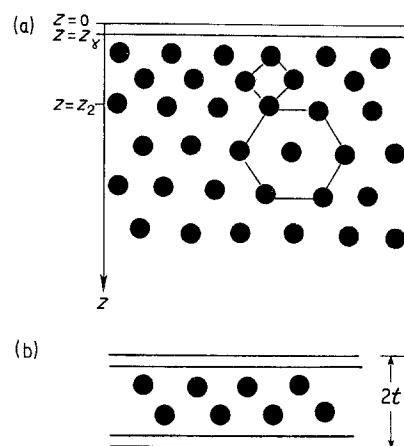


Figure 1 Schematic illustration of the idealized structures expected to occur as a function of distance from the surface in block copolymer systems. (a) Surface region of a bulk sample, (b) structure expected in a thin-film sample.

surface itself. As well, the component located at the surface would be the one which minimizes the surface energy associated with the structure. For a block copolymer consisting of blocks denoted A and B, if the two blocks have very different surface energies, i.e.  $\gamma_B \gg \gamma_A$ , then it would be expected that the block copolymer should arrange itself so that Block A is preferentially located at the free surface. The depth to which this preferential surface segregation occurs is denoted  $z_1$  in Fig. 1a, and will be a function of both the radius of gyration of the A block, as well as the relative volume fraction of the A block compared to that of the B block. (That is, if the B block is very much greater in size than the A block, the need to maintain consistency of segmental density on both sides of the A–B interface may be most easily satisfied by thinning and spreading out of the A layer.) For block copolymers of moderate molecular weight the depth of this surface region would be at most a few tens of nanometres.

Consideration of the interplay between the two surface energies (and the volume fractions of the two blocks) leads to some intriguing possibilities. For example, if  $\gamma_A$  is only slightly smaller than  $\gamma_B$  in magnitude, and the A block is the minority component, it may be possible to suppress preferential surface segregation. That is, the free-energy reduction obtained by preferential segregation of the A block to the surface (with the attendant chain deformation penalties) may be smaller than the free-energy reduction attained by having the A block arrange itself into microdomains. Such ideas can be investigated by varying the molecular weight and composition of the two blocks, or by using substrates (in place of the free surface) that possess different surface energies. A second possibility for the structure of the surface region of a block copolymer is the existence of a non-phase segregated region. An example of such a phenomenon has already been noted in the phase segregation in thin films of polymer blends, where, as the film thickness decreases, the film becomes more stable towards decomposition [22].

Adjacent to the region displaying the preferential surface-segregated or non-phase-segregated behaviour,

will be a region in which the block copolymer microdomains have formed. These microdomains would, if free of surface constraints, order into the lattice structures observed in bulk samples. However, the existence of the surface necessarily imposes constraints that must be addressed. It might be expected that the microdomain lattice plane with the lowest associated "surface energy" would be oriented parallel to the free surface (see e.g. [23]). Such a situation would have important implications in terms of producing structures with specific microdomain lattice orientations if substrates and copolymers with appropriate surface energies were chosen. In addition, it is conceivable that due to the different constraints imposed upon the chains at the surface compared to the constraints in the bulk, the "interplanar" lattice spacing between the surface and adjacent layer of microdomains may have a different value from that observed in the bulk. This situation would correspond to the well-known analogue in solid-state structures where the interplanar spacing of some metals is known to be different for the surface planes compared to the equilibrium interior spacings (see e.g. [24]).

Anticipating our own results, alternatively, this region of microdomain ordering may undergo wholesale changes in structure due to the proximity of the surface. For example, in the case of spherical micelles that order on to a bcc lattice in the bulk, the micelles may order into a structure with a different symmetry in the first few layers nearest the surface. Such a situation is schematically represented in Fig. 1a. The surface-ordered region, located up to a depth of  $z_2$  in Fig. 1a, would be expected to extend to a depth of about one repeat unit of the ordered microdomain lattice parameter. The structure of this surface-ordered region of microdomains would undergo a transformation to the three-dimensional bulk-ordered structure as one proceeds into the interior of the structure.

Surface effects should be readily manifested in thin polymer films. The situation can be idealized as shown in Fig. 1b, where the block copolymer has been confined between two parallel infinite surfaces a distance  $2t$  apart. When  $2t$  is very small, preferential segregation of the block with the lowest surface energy to the surface should be observed in the film; or a mixed, single-phase state may be observed. As  $2t$  is increased, a "two-dimensional" structure should be observed, corresponding to the "surface ordering" of microdomains. Finally, a transition corresponding to the bulk three-dimensional structure should be observable at sufficiently large film thickness.

The use of thin-film techniques allows the investigation of other interesting phenomena as well. First, a thin film can easily be formed on different substrates to investigate the effect of varying the interface surface energies on the observed block copolymer structures. Second, a film can also be produced between two identical substrates to produce a film possessing mirror symmetry across the midplane of its structure due to the symmetry of the boundary conditions. In addition, by adding homopolymer to copolymer samples, the preferential segregation of the homopolymer constit-

uent, depending on such factors as surface energy and molecular weight, can easily be studied. Finally, it is realized that in the process of casting films, an asymmetrical structure is expected to arise due to the escape of the solvent through only one of the surfaces. This particular asymmetry may be eliminated by a post-annealing process. By eliminating or modifying the annealing procedure, the nature and effect of such asymmetric evaporation should also be easily studied using thin films of block copolymers.

In this paper, we investigate the influence of surface constraints on block copolymer ordering. The approach used to study this phenomenon is to confine the block copolymer to a film of thickness that is of the same order as the scale over which phase segregation takes place. The domain morphology that develops reflects the "two-dimensional" nature of the film. To study the influence the surface has on the microdomain morphology, block copolymers with various volume percentages of the minority component were used; this allows the detailed effects on sphere, cylindrical and lamellar morphologies to be investigated. A region in which the microdomain separation does not take place is evidenced in the thinnest regions. In addition, the transition from these thin-film domain structures to those found in the bulk as the thickness of the films is increased is investigated. The increase in thickness of the film is found not to be continuously variable but instead is quantized, reflecting the presence of the discrete microdomains, which in turn is determined by the size of the constituent blocks present.

## 2. Experimental procedure

### 2.1. Sample synthesis

The characteristics of the styrene-butadiene diblock copolymers are given in Table I. Synthesis was performed via the usual anionic technique employed for styrene-butadiene block copolymers [25]. Purified butadiene (or styrene) monomer, benzene solvent, and sec-butyllithium initiator are allowed to react completely at 30° C under a high vacuum, after which a small sample is removed from the reaction flask for later analysis. The second monomer is then added to the reactor and allowed to react completely, after which the reaction is terminated by addition of degassed methanol.

### 2.2. Molecular characterization

The molecular weight distributions of the block copolymers and the samples removed from the reactor after polymerization of the first block were obtained with a Waters 150C gel permeation chromatograph (GPC) which had been calibrated with polystyrene standards.

TABLE I Molecular characteristics of poly(styrene butadiene) block copolymers

Sample designation	$M_n$ (kg mol <sup>-1</sup> )		PS (wt %)	PS (vol %)
	PS	PB		
SB 1	56.6	10.9	83.9	81.8
SB 2	22.2	9.0	71.2	68.2
SB 3	42.3	45.0	48.2	44.7
SB 4	20.5	20.5	50.0	46.5

In addition, the block copolymer compositions were determined by UV absorption in tetrahydrofuran at a wavelength of 260 nm. The molecular weights of the majority-component blocks were then calculated from the minority-component block molecular weight obtained from GPC and the composition determined by UV analysis. The characterization is presented in Table I. Although the microstructure of the polybutadiene was not determined, typical microstructures obtained from such anionic polymerizations contain approximately 90% mixed 1,4 *cis* and *trans* and 10% 1,2 addition.

### 2.3. Structural characterization

The films were produced by placing drops on a carbon-coated glass slide from a very dilute solution ( $\sim 0.05$  wt/vol %) of the particular block copolymer in toluene, a non-preferential solvent. Upon evaporation of the toluene, extremely thin isolated regions of the copolymer are left on the slide. These specimens were then annealed under vacuum at 120°C for several hours; this procedure ensures that any residual solvent is removed from the polymer and that the sample is allowed to attain its equilibrium morphology. (Some samples were not subjected to the annealing process, so that the effects this procedure had on the long-range order of the microdomains could be determined.) After annealing, the carbon coating was separated from the glass slide by immersing the slide in a distilled water bath. The carbon layer (which acts as substrate for the polymer) floats on the water bath, allowing the polymer and its carbon support to be picked up on standard mesh TEM grids.

A JEOL 100CX electron microscope operated at 100 kV was used to examine the structure of the samples. To enhance the contrast between the butadiene and styrene phases, the samples were stained by exposure to OsO<sub>4</sub> vapours for 4 h prior to observation by electron microscopy. The PB domains are stained by the OsO<sub>4</sub> and appear darker in the TEM images than the polystyrene. A side-entry goniometer and tilt-rotate specimen holder allowed the sections to be

rotated  $\pm 180^\circ$  in the plane of the specimen and tilted about any chosen axis by  $\pm 60^\circ$ .

Local variations in the thickness of the sample lead to regions on the electron image plate containing different optical densities which can be quantitatively analysed by microdensitometry. The optical density of the image in regions of interest is measured, as well as the optical density of the substrate; these values allow the relative mass thicknesses of the different regions to be determined [26]. Owing to the extreme thinness of the samples, uniform staining of the phases by the OsO<sub>4</sub> can be assumed. Furthermore, images of lamellar samples (of different thicknesses) in which the electron beam travels through the domains so that the domains are projected upon each other come about by the scattering of the electron beam from the same proportion of PS to PB. Thus the analysis of the relative local mass thickness allows the relative thickness of the sample in these regions to be determined.

## 3. Results

### 3.1. Structures involving lamellar microdomains

Two orientations of the microdomains are observed in the lamellar samples. Fig. 2 shows an unannealed droplet of Sample SB3 containing 55.3 vol % PB in which the lamellae are oriented perpendicular to the film substrate. The other dominant morphology observed is one in which the lamellae lie parallel to the plane of the substrate, as shown for example in Fig. 3 for Sample SB4 (53.5 vol % PB). For this latter orientation, a layering or stacking of lamellae parallel to the plane of the substrate is evident as an abrupt increase in image contrast due to step increases in sample thickness. For specimens containing cylindrical or spherical microdomains, the only effect of annealing was to improve the long-range order. However, for the lamellar samples, the annealing process could change the dominant orientation. Before annealing, roughly half the droplets made from the lower molecular weight polymer (SB4) and all the droplets made from polymer SB3 revealed the "end-on" appearance in which the lamellae were oriented perpendicular to the substrate. After annealing, the lamellae lay parallel to

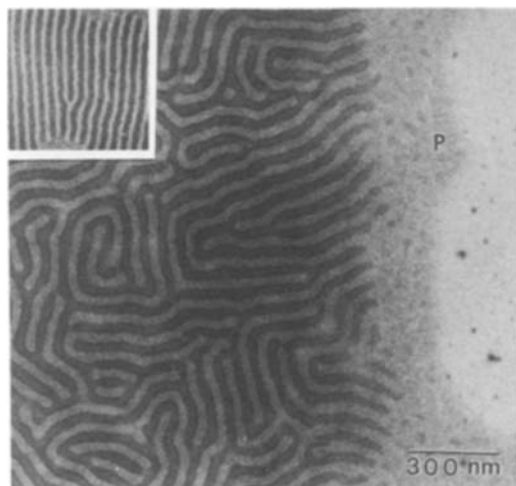


Figure 2 Electron micrograph of an unannealed sample containing 55 vol % PB. The lamellae are seen perpendicular to the film surface. Inset: a "dislocation" observed in a well-ordered region.

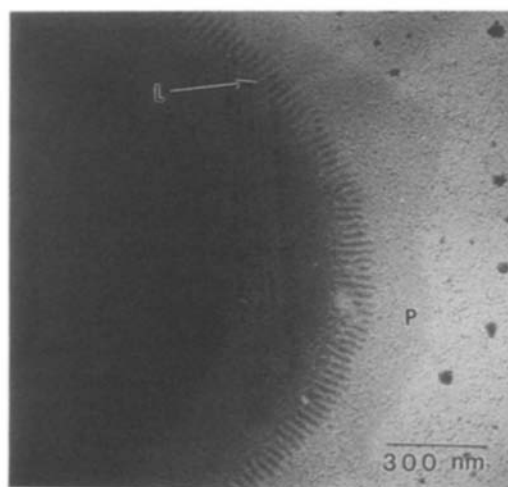
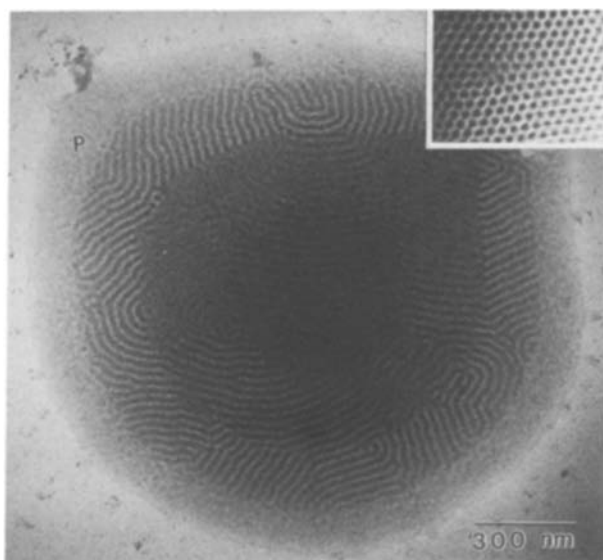


Figure 3 Electron micrograph of a sample containing 54 vol % PB. The lamellae are seen lying in the plane of the film surface.



*Figure 4* Electron micrograph of a sample containing 32 vol % PB. Cylindrical domains are readily apparent. Inset: electron micrograph in the thickest region of a 32 vol % PB sample.

the substrate except for occasional end-on regions in the higher molecular weight SB3 sample.

From micrographs with the end-on lamellar orientation, the PS and the PB regions have widths of 23.9 and 28.1 nm, respectively, for Sample SB3, and widths of 16.7 and 19.7 nm for Sample SB4. Excellent agreement is found between these relative widths and the volume percentage of the constituent blocks present (see Table I). This agreement indicates that any swelling of the PB phase due to the staining by the  $\text{OsO}_4$  is small. Also noted is a peripheral region at the edge of the drop, denoted P in the micrograph (Fig. 2). In this region the segregation of the block copolymer into lamellar microdomains appears not to have taken place.

### 3.2. Cylindrical microdomain ordering

When the volume percentage of polybutadiene is decreased to 32, cylindrical microdomains are observed. In thin droplets, these are observed as an array of parallel rods in the plane of the substrate (Fig. 4). The PB cylinders have an average diameter of 14.8 nm, and nearest neighbours are separated by a distance of 27.5 nm. Again, there is a stacking of layers in the thicker regions of the droplet, as well as a region located in the thinnest periphery of the film that displays a lack of well-developed phase segregation.

The assertion that the domains are cylindrical rather than lamellar follows from two pieces of evidence. First, in the thickest parts of some droplets, as shown in the inset of Fig. 4, there are grains that have an end-on projection where a hexagonal-packed array of the cylinders is clearly evident. (It should be emphasized that this end-on orientation was never observed in regions less than approximately 150 nm in depth; thus this image is dominated by the interior structure of the droplet.) The second piece of evidence follows from a tilting experiment on a droplet containing two layers of cylinders: Fig. 5 shows a droplet that has a double layer of cylinders in its thickest region. In the

central region, one layer appears to be stacked upon the other. The evidence that cylindrical microdomains are present is confirmed by performing a tilting experiment as shown in Fig. 5. Here, the projection through a droplet containing a two-layer region is viewed at  $+20^\circ$ ,  $0^\circ$ ,  $-30^\circ$ . Note that cylinders can be clearly distinguished when viewed at angles of  $+20^\circ$  and  $-30^\circ$ ; for these cases the cylinders in the top layer project directly upon those below it. However, when the structure is viewed normal to the film surface ( $0^\circ$ ), the polybutadiene cylinders of the top layer eclipse the polystyrene matrix between the cylinders in the bottom layer. Thus very poor contrast is observed. (Also note that in this tilt series, the outer, single layer of cylinders remains in sharp contrast at all angles, proving that this region is indeed a single layer of cylinders.)

### 3.3. Spherical microdomain ordering

The morphology of a typical film droplet made from polymer SB1 (18 vol % polybutadiene) is shown in Fig. 6. Spherical microdomains of the polybutadiene are observed. (It should be noted that cylindrical domains viewed end-on would also appear spherical. To address this question, tilting experiments were performed to conclusively show that these domains were indeed spherical in nature.) The polybutadiene domains have an average diameter of 18.0 nm. The microdomains arrange themselves to yield a hexagonally ordered grain, with an average distance between domains of 37.5 nm. As was already observed for the cases of lamellar and cylindrical microdomains, at the edge of the droplet there is a region in which there is a change in the segregation behaviour of the block copolymer. Although there is some evidence for the formation of a few very poorly developed spherical microdomains in the interior area of this peripheral region, overall it is generally characterized by uniformity in image contrast.

When thicker droplets were investigated, abrupt step increases in thickness were observed proceeding in from the edge of the droplet. These increases in thickness were accompanied by changes in the projected microdomain structure as shown in Fig. 7. Thus, similar to films that possessed cylindrical or lamellar microdomains, films which had spherical micelles also present a discrete layering of the ordered domain structures.

## 4. Discussion

Before discussing each of the microdomain structures individually, some comments on features common to all three are in order. One of the most notable items observed in all specimens, regardless of their composition, was the region at the periphery of the droplets that did not contain well-developed microphase segregation (this region is denoted P in the micrographs), clearly distinguished from the rest of the droplet structure by its uniform contrast. It should be pointed out that this region may envelop the entire droplet as illustrated schematically in Fig. 8. However, in a situation where a layer which appears uniform in contrast in the TEM is superimposed on top of a layer containing microdomains, electron micrographs

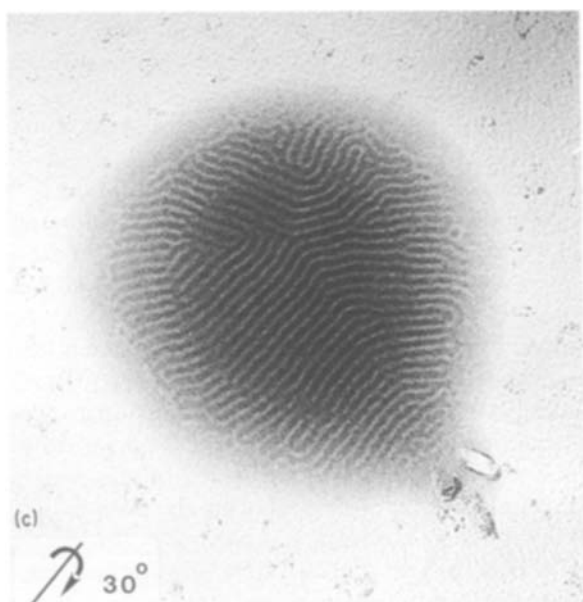
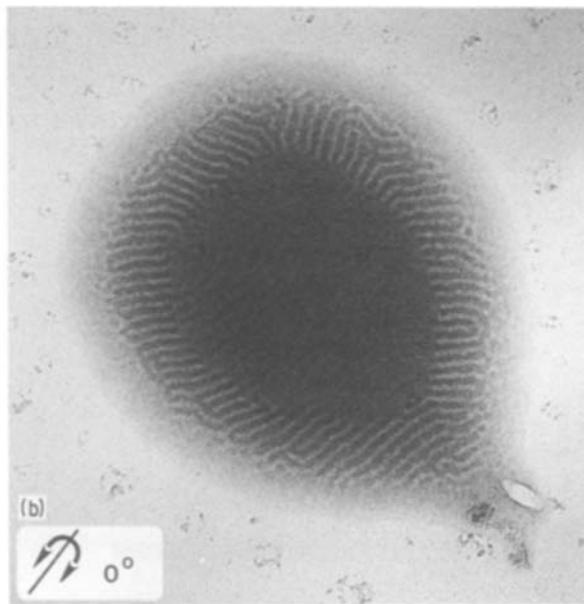
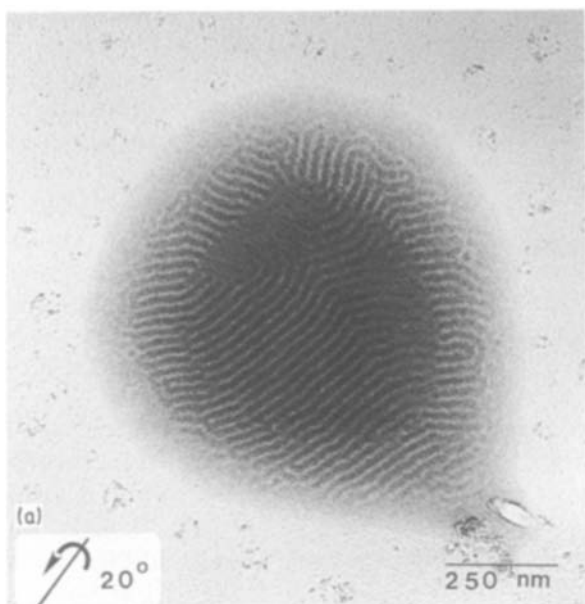


Figure 5 Electron micrographs of the same region in a film made from a sample containing 32 vol % PB. (a) Viewed at an angle of  $+20^\circ$  to the perpendicular. (b) Viewed perpendicular to the film substrate ( $0^\circ$  tilt). (c) Viewed at an angle of  $-30^\circ$  to the perpendicular.

of the projected object would be dominated by the contrast of the domain structures; thus at present it is not possible to determine if this region completely encapsulates the droplet or only occurs at the periphery.

There are two possible ways in which this uniform contrast structure can be accounted for. The first

explanation is that this region represents a non-phase-segregated polymer mixture ((i) in Fig. 8). Studies of the phase segregation behaviour of polymer blends in thin films have shown that as the film thickness decreases, the film becomes increasingly more stable towards phase segregation [22]. Note that since such a region will still contain PB, it would be stained by the  $\text{OsO}_4$  and appear darker when compared to a region of pure PS. Thus, if a bulk sample containing such a surface region was cross-sectioned, it would reveal a stained layer at the surface that might be interpreted as a pure polybutadiene layer.

An alternate explanation of the peripheral structure would be if the polymer molecules arrange themselves so that a particular component block is exposed to the top, bottom, or both surfaces preferentially. Thus, this region may represent a bilayer of the PS–PB blocks, or perhaps even a tri-layer with one component sandwiched in between two layers of the other component, as illustrated in Fig. 8(ii). Hasegawa and Hashimoto's recent observation [21] that one polymer preferentially

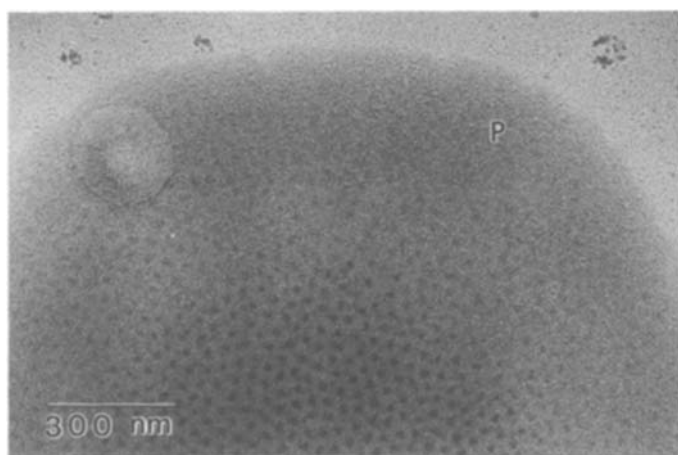


Figure 6 Electron micrograph of thin droplet of a sample containing 18 vol % PB. A hexagonal array of spherical microdomains of PB is readily apparent.

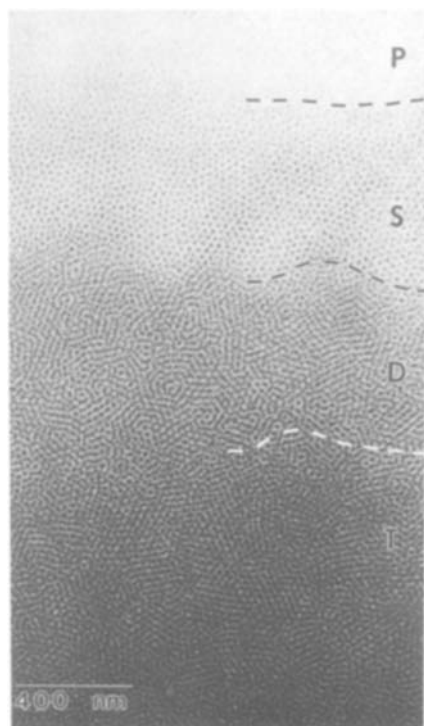


Figure 7 Electron micrograph of the edge of an 18 vol % PB film of increasing thickness. The stacking of layers has been partially outlined.

segregates to the surface in bulk samples suggests this interpretation. The driving force for such a preferential segregation of one block to the surface(s) would be to decrease the surface energy of the film. Thus, the block with the lowest surface energy (in this case the PB) would be expected to be located at the surface.

This latter interpretation of the peripheral structure is supported by the observation that the peripheral regions are very uniform in contrast in the EM images. This observation indicates that this region does not gradually decrease in thickness as the edge of the drop is approached, but is of uniform depth. If the peripheral regions represented a mixed phase, it would be expected that this region would not be restricted to have any particular uniform value of thickness; rather the thickness should decrease toward the edge of the droplet. On the other hand, a situation where one block preferentially segregated to the surface would mean that the thickness of the peripheral region would be discrete, and determined by the molecular weights of the constituent blocks.

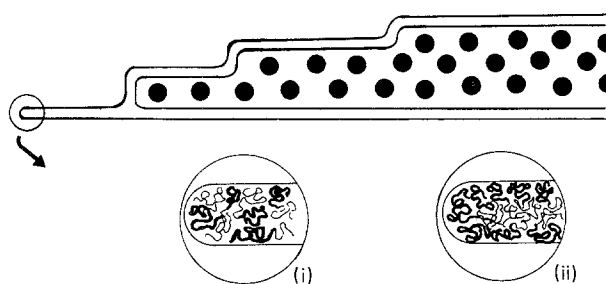


Figure 8 Schematic diagram showing the edge of a droplet. Two possibilities are shown for the structure present in the peripheral region: (i) Miscible, single-phase region or (ii) preferential segregation of one of the blocks to the surface.

Another observation deserving comment is the step increases in thickness of the droplets. The presence of layers has been observed previously using electron microscopy replication techniques on solvent-cast bulk films of diblock SB copolymers exhibiting lamellar morphology [18, 19], as well as by optical techniques in ternary block copolymer-solvent systems [20]. However, the nature of the phenomenon giving rise to this surface structure was not investigated in detail. In the current set of experiments, this phenomenon was observed in all the samples except those specimens in which the lamellae were oriented perpendicular to the substrate surface.

#### 4.1. Ordering of lamellae

Two types of orientation were encountered when compositions that form lamellar microdomains were studied. The change in the dominant microdomain orientation upon annealing from being one in which the lamellae are arranged perpendicular to the substrate to one in which they lie parallel to the substrate indicates that this latter orientation represents the equilibrium arrangement. This changeover in orientation occurs to allow the component with the lower surface energy access to the external surface. The electron micrographs were analysed by microdensitometry to determine the relative mass thickness of the various regions in the droplets with the layered morphologies. The incremental increase in mass thickness (i.e. depth) of each layer is approximately the same except for the outermost peripheral layer. This region is only 1/4 to 1/2 as thick as the interior layers. This suggests that the outermost layer possess a different morphology and probably represents the peripheral regions found in the cylindrical- and spherical-domain samples. The thickness of this peripheral region is also consistent with observations made by Hasegawa and Hashimoto on the surface structure of lamellar samples [21]. Their results on specimens that had been cross-sectioned perpendicular to the exterior surface revealed a surface layer of PB which was 1/2 as thick as the internal PB lamellar domains.

At the edges of some of the interior layers, the edge-on lamellar orientation was sometimes observed. As shown by the arrow denoted *L* in Fig. 3, the lamellae initially started to form in an orientation perpendicular to the substrate surface (edge-on); however, after a short distance, the orientation of the lamellae changed abruptly to lie parallel to the plane of the substrate (face-on). The initial edge-on orientation of lamellae might be expected to occur as a consequence of the rapid evaporation of the solvent. As the solvent evaporates, the region of the droplet plasticized by the solvent will be shrinking radially. Thus the segregating lamellae are growing perpendicular to the receding solvent front. As discussed above, a changeover in orientation may result since the face-on orientation allows the lower-energy component access to the external surfaces. The boundary region between two sets of lamellae that are oriented perpendicular to each other (a 90°-twist grain boundary) may be described by a minimal surface [27]. Such a surface minimizes the interfacial area between the unlike phases.

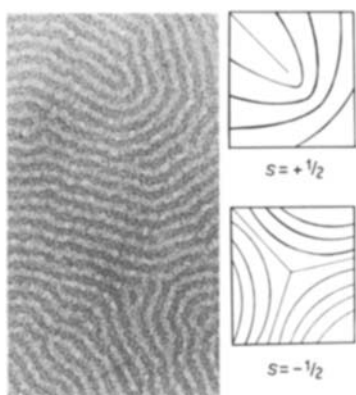


Figure 9 The nematic-like ordering in cylindrical microdomains in a single-layer region showing the presence of  $s = +1/2$  and  $s = -1/2$  disclinations.

#### 4.2. Ordering of cylindrical microdomains

The stacking of layers of cylindrical microdomains is shown in Figs 4 and 5. The cylinders prefer to lie parallel to each other in a given layer, and have their long axes oriented perpendicular to the droplet edge. This leads to a sectioning of the interior of the droplets into “orientation domains”. The cylinders within each of these grains are observed to be parallel, but the grains themselves are disoriented with respect to each other. The orientation of the cylinders changes continuously as the grain boundary is crossed. An analogous morphology has been recently observed in nematic liquid-crystalline polymers and can be described as translationally parallel object fields containing arrays of disclinations [28]. Fig. 9 shows the presence of  $s = -1/2$  and  $s = +1/2$  disclinations (see insets of Fig. 9). (The observation of a “dislocation” in a lamellar sample is shown in the inset of Fig. 2.) These thin-film droplet specimens are an ideal means by which to study defects in mesophase microstructures [29].

A remarkable registration of cylinders between layers is also observed in these samples. It was noted that in multiple-layer drops, the upper layers of cylinders positioned themselves on top of the inter-cylinder

region of the layer below (this stacking is illustrated in Fig. 8). Thus, the region containing two layers of cylinders was generally one of poor contrast. Such a registration between layers would be expected to minimize the deformation of the corona chains in the interstitial space. This specific positioning of the cylinders in each subsequent layer leads to a regular ordering of the microdomains in the direction perpendicular to the substrate surface. It is easy to envision how such a stacking of layers leads to a regular three-dimensional structure.

#### 4.3. Spherical microdomain ordering

Observations of the sample containing 18 vol % PB (Figs 6 and 7) reveal the peripheral uniform-contrast region, then a single layer of hexagonally ordered spherical microdomains in the droplet interior, followed by stacked layers of these hexagonally-packed sheets. Fig. 10a schematically illustrates the situation when two such sheets are stacked, one upon the other. The top layer is offset from the bottom layer such that the spheres in the upper layer are located over the interstitial sites of the lower layer. As illustrated in Fig. 10a, viewing the structure at an angle of  $35^\circ$  (i.e. along the  $[\bar{2}203]$  direction of a hexagonally close-packed structure) results in the top layer of spheres projecting directly on to the bottom layer. When such a region containing two layers (e.g. denoted D in Fig. 7) is observed normal to the substrate surface, no easily characterized domain packing pattern is discernible (see Fig. 11a). However, when the sample has been tilted through an angle of approximately  $30^\circ$  (Fig. 11b), the same region reveals a projected structure of well defined, ordered spheres.

The offset of the top layer of micelles is expected from a simple model of stacking layers of micelles to fill space, and at the same time minimizing the unfavourable deformation of the corona chains to fill the interstitial space. The long-range registry between layers containing spherical microdomains is much poorer compared to the case of cylindrical microdomain stacking. This follows from the fact that in a

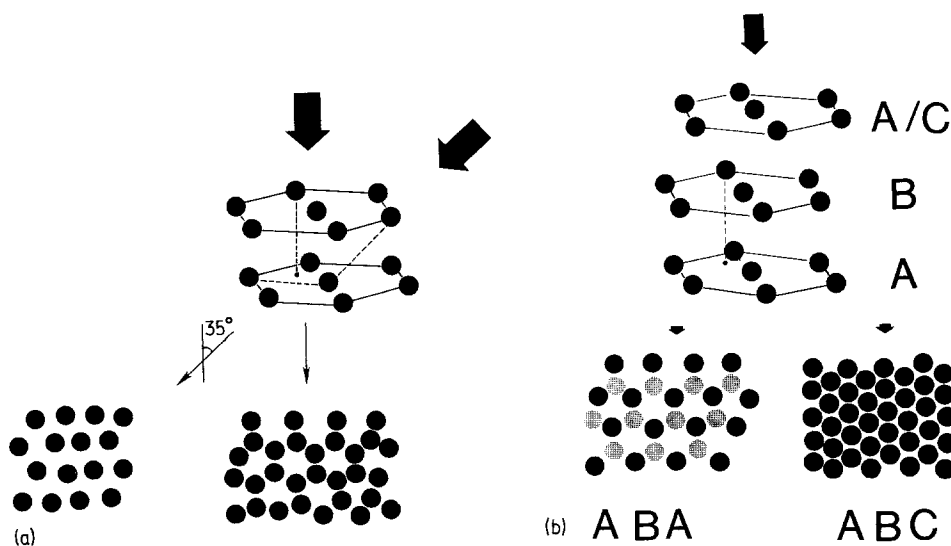


Figure 10 (a) Stacking of two layers of spheres in close-packed planes, and the resulting projected image when viewed perpendicular to the planes, or at a tilt angle of  $35^\circ$  to the perpendicular. (b) Stacking of three layers of spheres in close-packed planes.

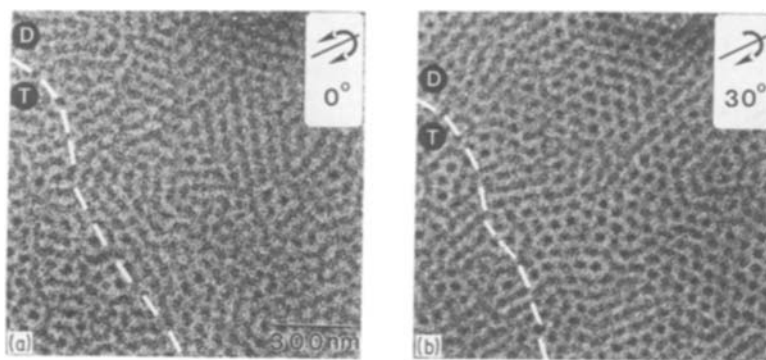


Figure 11 Electron micrographs of the same region in a film made from a sample containing 18 vol % PB. (a) Viewed perpendicular to the film substrate ( $0^\circ$  tilt). (b) Viewed at an angle of  $30^\circ$  to the perpendicular.

two-dimensional hexagonally packed lattice of spheres, there are two sets of equivalent interstitial “sites”. Each set of sites can act to locate a two-dimensional hexagonally packed layer directly on top of itself. Therefore in the case of spherical microdomain ordering, the top layer has a choice of two sites over which to be located. The extra degree of freedom for spherical micelle ordering is absent in the case for cylindrical microdomains where there is only one favoured way for the upper layer to locate over the lower; and that is for the top layer of cylinders to be located over the inter-cylindrical regions of the bottom layer.

Stacking hexagonally packed layers can also be used to explain the observed structure in the region of the droplet containing three layers (Region T of Fig. 7). In this region, there are areas of poorly defined structure, as well as projections of what appear to be regions with well defined, singular micelle cores. (These features are shown in detail in the lower part of Fig. 11a). The indistinct nature of the pattern observed in this thick region did not change markedly when samples were tilted (Fig. 11b). In the stacking of hexagonally packed layers, the two equivalent interstitial sites in each hexagonally packed plane can be used to obtain the familiar stacking sequences ABABAB of hexagonal close-packed structures, or ABCABCABC of face-centred cubic structures (Fig. 10b). In stacking several layers of micelles, the corona chains interact only with the layer immediately adjacent to them. Thus even though the middle layer may have a relationship to either the bottom or top layer on a local level, over large areas these upper and lower layers no longer have any special relationship to each other. When they happen to stack on over each other in a particular region, the  $[0001]$  projection through two layers of micelle cores gives rise to regions in the image containing well defined, single micelle cores.

The above results on stacking two-dimensional layers are consistent with experiments that have investigated the structure of solutions containing latex particles [30–33]. In these systems, it was observed that the outermost layer generally consisted of a two-dimensional hexagonally packed array. Depending on the concentration or the presence of charge, these close-packed layers were found to stack in either a random manner, or in a regular fashion to yield an fcc lattice. In our present system, the increase in mass thickness with increasing sample thickness precluded determining the equilibrium “bulk” structure. From other studies however [4, 15], it is known that in such

bulk samples, the micelles order on to a bcc lattice. The ordering on to this lattice is a consequence of the desire to minimize the unfavourable deformation of corona chains in the interstitial space between micelle cores (a constraint absent in the latex systems).

## 5. Conclusions

The structures present in thin films of block copolymers reflect the two-dimensional nature of the films. In observing the structure in thin-film droplets as a function of diblock composition (and hence microdomain type), several distinct regions were observed. First, in the thinnest peripheral region of the droplets, a region of uniform contrast, when viewed by TEM, was observed. The consistency of the thickness of this peripheral region provides evidence that preferential surface segregation of the block with the lowest surface energy takes place in order to minimize the surface energy of the overall structure. The observation of such a region in these thin films indicates that such a region may be present on the surface of bulk samples.

For block copolymers exhibiting spherical or cylindrical microdomain morphology, a single layer of microdomains was observed in the thicker regions of the film adjacent to the peripheral region. In the case of spherical microdomains, an ordering of the domains on to a hexagonal lattice was observed, as it allows for the most efficient packing of the microdomains in two dimensions. The cylindrical domains arrange themselves into grains in such a way that their long axes are perpendicular to the edge of the droplet. Within each grain, the cylinders are aligned parallel to each other, and parallel to the film surface. In the thicker part of the film droplets, for samples exhibiting spherical and cylindrical microdomain morphology, a stacking of these two-dimensional layers was observed. For the films exhibiting spherical domain structure, adjacent hexagonally packed layers were offset from each other. However, there was no ordered stacking sequence for these samples; rather it appeared that the hexagonal layers, while precisely offset, stacked randomly upon each other. In the case of cylindrical domains, the layers of cylinders arranged themselves such that the cylindrical domains would lie parallel to (but transversely shifted from) those in the adjacent layers.

For the lamellar samples two orientations of the lamellae were observed. In one orientation, the lamellae were oriented perpendicular to the film surface. However, upon annealing, this orientation was found less frequently, and the other orientation in which the

lamellae were "stacked" parallel to the film surface was found to be the dominant structure. This latter structure is favoured as it allows the component with the lowest surface energy access to the external surfaces. The stacking of layers which led to the terraced nature of the surfaces for all the microdomain structures investigated indicates that the surfaces of bulk samples may be terraced in a similar manner.

The morphologies observed in the thinnest parts of the droplets arise due to the additional constraints imposed on the various domain structures from the proximity of the external surfaces. As one proceeds into the thicker regions of the droplets, two-dimensional and then three-dimensional ordering of microdomains takes place. These well-defined structures obtained in block copolymer thin films may have some unique uses in such applications as microlithography and membrane technology. They also present a convenient way to test models of block copolymer systems. These experiments have important implications in understanding the structures at and near the surfaces of bulk samples.

### Acknowledgements

Financial support from the National Science Foundation, Grant DMR 84-06079, and the University of Massachusetts Institute for Interface Science (supported by IBM) is gratefully acknowledged. The authors also thank Dr D. J. Kinning of 3M Company for useful discussions, and the NSF Materials Research Laboratory at the University of Massachusetts for facilities.

### References

1. G. KÄMPF, M. HOFFMAN and H. KRÖMER, *Ber. Bunsenges. Physik. Chem.* **74** (1970) 851.
2. G. E. MOLAU, in "Block Copolymers", edited by S. L. Aggarwal (Plenum, 1970).
3. E. PEDEMONTE, A. TURTURRO, V. BIANCHI and P. DEVETTA, *Polymer* **14** (1973) 145.
4. F. S. BATES, R. E. COHEN and C. V. BERNEY, *Macromolecules* **15** (1982) 589.
5. T. HASHIMOTO, M. FUJIURA and H. KAWAI, *ibid.* **13** (1980) 1660.
6. R. J. ROE, M. FISHKIS and V. C. CHANG, *ibid.* **14** (1981) 1091.
7. R. W. RICHARDS and J. L. THOMASON, *Polymer* **22** (1981) 581.
8. *Idem*, *Macromolecules* **16** (1983) 982.
9. B. R. M. GALLOT, *Adv. Polym. Sci.* **29** (1979) 85.
10. D. J. MEIER, in "Block and Graft Copolymers", edited by J. J. Burke and V. Weidss (Syracuse University Press, Syracuse, 1973).
11. E. HELFAND and Z. R. WASSERMAN, in "Developments in Block Copolymers - I", edited by I. Goodman (Applied Science, New York, 1982).
12. L. LEIBLER, *Macromolecules* **13** (1980) 1602.
13. E. L. THOMAS, D. B. ALWARD, D. J. KINNING, D. C. MARTIN, D. L. HANDLIN Jr and L. J. FETTERS, *ibid.* **19** (1986) 2197.
14. H. HASEGAWA, H. TANAKA, K. YAMASAKI and T. HASHIMOTO, *ibid.* in press.
15. E. L. THOMAS, D. J. KINNING, D. B. ALWARD and C. S. HENKEE, *ibid.* **20** (1987) 2934.
16. A. K. RASTOGI and L. E. ST PIERRE, *J. Colloid Interf. Sci.* **31** (1969) 168.
17. H. R. THOMAS and J. J. O'MALLEY, *Macromolecules* **12** (1979) 323.
18. E. VANZO, *J. Polym. Sci. A-1* **4** (1966) 1727.
19. E. B. BRADFORD and E. VANZO, *ibid.* **6** (1968) 1661.
20. J. C. WITTMANN, B. LOTZ, F. CANDAU and A. J. KOVACS, *J. Polym. Sci., Polym. Phys. Edn* **20** (1982) 1341.
21. H. HASEGAWA and H. HASHIMOTO, *Macromolecules* **18** (1985) 589.
22. S. REICH and Y. COHEN, *J. Polym. Sci., Polym. Phys. Edn* **19** (1981) 1225.
23. D. P. WOODRUFF, "The Solid-Liquid Interface" (Cambridge University Press, 1973).
24. Y. TAKEISHI and K. HIRABAYASHI, in "Lattice Defects in Semiconductors", edited by R. R. Hasiguti (University of Tokyo Press, 1968).
25. L. J. FETTERS, *J. Polym. Sci. C* **26** (1969) 161.
26. B. D. LAUTERWASSER and E. J. KRAMER, *Phil. Mag.* **39A** (1979) 469.
27. E. L. THOMAS, D. M. ANDERSON, C. S. HENKEE and D. HOFFMAN, Science (submitted).
28. B. A. WOOD and E. L. THOMAS, *Nature* **324** (1986) 655.
29. S. L. HUDSON, C. S. HENKEE and E. L. THOMAS, in preparation.
30. A. KOSE, M. OZAKI, K. TAKANO, Y. KOBAYASHI and S. HACHISU, *J. Colloid Interf. Sci.* **44** (1973) 330.
31. N. ISE, T. OKUBO, M. SUGIMURA, K. ITO and H. J. NOLTE, *J. Chem. Phys.* **78** (1983) 536.
32. T. YOSHIMYAMA, *Polymer* **27** (1986) 827.
33. T. YOSHIYAMA, I. SOGAMI and N. ISE, *Phys. Rev. Lett.* **53** (1984) 2153.

Received 27 May  
and accepted 24 July 1987